J Nanopart Res (2014) 16:2547
DOI 10.1007/s11051-014-2547-3

RESEARCH PAPER

Palladium(0) nanoparticles supported on hydroxyapatite nanospheres: active, long-lived, and reusable nanocatalyst for hydrogen generation from the dehydrogenation of aqueous ammonia–borane solution

Yasar Karatas · Mehmet Yurderi · Mehmet Gulcan · Mehmet Zahmakiran · Murat Kaya

Received: 16 March 2014 / Accepted: 1 July 2014 / Published online: 15 July 2014

Abstract Among the solid materials considered in the chemical hydrogen storage, ammonia–borane (NH_3-BH_3) appears to be one of the promising candidates as it can release hydrogen throughout hydrolysis in the presence of suitable catalyst under mild conditions. Herein we report, for the first time, the preparation and characterization of palladium(0) nanoparticles supported on nanohydroxyapatite and their catalytic use in the hydrolysis of ammonia–borane under air at room temperature. These new palladium(0) nanoparticles were generated in situ during the catalytic hydrolysis of ammonia–borane starting with palladium(II) immobilized nanohydroxyapatite. The preliminary characterization of the palladium(0) nanoparticles supported on nanohydroxyapatite was done by the combination of complimentary techniques, which reveals that the formation of well-dispersed Pd(0)NPs nanoparticles (1.41 ± 0.52 nm) on the surface of hydroxyapatite nanospheres (60–150 nm). The resulting palladium nanocatalyst achieves hydrogen generation from the hydrolysis of ammonia–borane with an *initial* turnover frequency value (TOF) of 11 mol H_2 mol^{-1} Pd × min at room temperature under air. In addition to their high activity, the catalytic lifetime experiment showed that they can also act as a long-lived heterogeneous catalyst for this reaction (TTON = 14,200 mol H_2 mol^{-1} Pd) at room temperature under air. More importantly, nanohydroxyapatite-supported palladium(0) nanoparticles were found to be highly stable against to leaching and sintering throughout the catalytic runs that make them isolable, bottleable, and reusable heterogeneous catalyst for the hydrolysis of ammonia–borane.

Keywords Palladium · Nanoparticles · Hydroxyapatite · Nanospheres · Catalyst · Ammonia–borane · Dehydrogenation

Y. Karatas · M. Yurderi · M. Gulcan · M. Zahmakiran (✉)
Department of Chemistry, Yüzüncü Yıl University, 65080 Van, Turkey
e-mail: zmehmet@yyu.edu.tr

M. Kaya
Department of Chemical Engineering and Applied Chemistry, Atilim University, 06836 Ankara, Turkey

Introduction

Hydrogen is a globally accepted clean energy carrier, which could solve the world energy problem and reduce the environmental pollution resulting from the "Hydrocarbon Economy" (Muradova and Veziroglu 2005). Hydrogen can be act as an environmentally cleaner energy carrier to end-users, particularly in transportation applications, without release of pollutants, or carbon dioxide at the point of end use (Turner 1999; Inter Academy Council 2007). Today, there have been serious endeavors in the development of safe and effective methods for the hydrogen storage, which is one of the key issues in the "Hydrogen Economy" (The National Academies Press 2004). On

account of this concern, there has been a rising concentration for the development of solid hydrogen storage materials that make available the combination of high volumetric/gravimetric storage capacity, adequate kinetics, reversibility, low cost, and low toxicity, as the majority of them are not practical in the existing high pressure and cryogenic hydrogen storage systems (Turner et al. 2008). In this context, various porous solid materials (Liu et al. 1999; Weitkamp et al. 1995; McKeown and Budd 2006; Rosi et al. 2003), where the hydrogen release and uptake can only be controlled by temperature and pressure, boron-containing metal hydrides (MBH_x) (Moussa et al. 2013), and boron–nitrogen (BN) adducts (Staubitz et al. 2010) have been considered and employed in the chemical hydrogen storage.

Amongst those, ammonia–borane (or borane–ammonia complex, NH_3BH_3) seems to be much better suited for this purpose due to its high gravimetric hydrogen capacity (19.6 wt%), that satisfies 2015 target of USA DOE (9 wt% hydrogen for a material to be practically applicable) (The National Academies Press 2004), non-toxicity, low molecular weight (30.7 g mol^{-1}), and propensity for including protic (N–H) and hydridic (B–H) hydrogens, which can be 'discharged' and 'recharged' in diverse chemical processes (Hamilton et al. 2009). Although, thermal dehydrogenation (Demirci et al. 2011), or metal-catalyzed thermolysis (Toche et al. 2012), dehydrocoupling (Jaska et al. 2003), and alcoholysis (Ramachandran and Gagare 2007) of ammonia–borane have been shown to induce the hydrogen generation, there is much concentration on the catalytic hydrolysis of ammonia–borane due to more favorable kinetics and requirement of milder reaction conditions (Demirci and Miele 2009; Jiang et al. 2010a, b; Jiang and Xu 2011; Sanyal et al. 2011). The catalytic hydrolysis of ammonia–borane generates 3 equiv. of H_2 per mole of ammonia–borane at room temperature under air (Eq. (1)) (Jiang et al. 2010a, b; Jiang and Xu 2011; Sanyal et al. 2011).

$$NH_3BH_3 + 3H_2O \xrightarrow[\text{at RT under air}]{\text{Catalyst}} NH_4BO_2 + 3H_2 \qquad (1)$$

In the face of complicatedness in recycling of the hydrolysis product borate anion, the hydrogen generation from the catalytic hydrolysis of ammonia–borane has important features that make it attractive for potential applications; (1) ammonia–borane is highly soluble in water at room temperature (33.6 g NH_3BH_3/100 g H_2O) (Stephens et al. 2007), (2) ammonia–borane has high stability against to self-hydrolysis in water, it hydrolyzes at appreciable rate only in the presence of active metal catalysts, (3) the hydrolysis of ammonia–borane is exothermic process ($\Delta H = -156$ kJ $\times$ mol^{-1}) (Bluhm et al. 2006). As mentioned above, an economically viable method for the regeneration of ammonia–borane hydrolysis product may be the ultimate barrier to its on-board application in hydrogen storage. Definitely, the methods for the efficient regeneration depend on the products, while the wide range of products shows greatly contradictory reactivities (Bluhm et al. 2006). The enthalpy calculations for the hydrolysis of ammonia–borane reveal that the regeneration under H_2 pressure is not energetically favorable in thermodynamics (e.g., -227 kJ mol^{-1} would be required for $NH_3BH_3 + H^+ + 3H_2O \rightarrow B(OH)_3 + 3H_2 + NH_4^+$) and the recycling of ammonia–borane from hydrolysis product was considered to be a multi-step process (Dixon and Gutowski 2005). Under the current technology, ammonia–borane and other chemical hydride with high storage capacity will require off-board regeneration, which adds to the complexity of the hydrogen storage system. However, these compounds can offer advantages for the fuel distribution system. The present fuel delivery system is based on transporting liquid hydrocarbons; converting this system to transport compressed or liquid hydrogen will be an expensive (Ogden 1999). Stable chemical hydrides can evade this problem, allowing for transportation of hydrogen using the existing transportation.

Since the hydrolysis of ammonia–borane occurs only in the presence of a suitable catalyst, many transition metals or their compounds have been tested as catalyst for this important reaction (Staubitz et al. 2010; Hamilton et al. 2009; Demirci and Miele 2009; Jiang et al. 2010a, b; Jiang and Xu 2011; Sanyal et al. 2011). Although, some homogeneous systems (Ciganda et al. 2010; Graham et al. 2010) had achieved reasonable activities, the current research has been directed towards the development of highly active, reusable, and long-lived heterogeneous catalysts because of their advantages including easy product/catalyst separation, catalyst recovery and their more simple synthesis routes with respect to homogeneous catalysts (Thomas and Thomas 1997). Expectedly, transition metal nanocatalysts provide better

performances than their classical heterogeneous counterparts (Zahmakiran and Özkar 2011) in the hydrolysis of ammonia–borane. However, the aggregation of metal nanoparticles into clumps is still the most important problems for the catalytic employment of metal nanocatalysts in this important reaction. It is well known that the aggregation of metal nanoparticles into bulk metal, albeit using the best stabilizing agents, leads to a significant lost in the catalytic performances of these catalysts (Zahmakiran and Özkar 2011). As an illustrative examples, in the recent studies of one of us, the momentous decreases in the catalytic activities of ruthenium(0) (Durap et al. 2009a, b) and rhodium(0) (Durap et al. 2009a, b) nanoparticles resulting from the aggregation of these initially well-stabilized nanoparticles during the hydrolysis of ammonia–borane have already been reported. In this context, the stabilization of metal(0) nanoparticles within the framework of water dispersible solid supports seems to be a logical way of preventing their aggregation into bulk throughout their catalytic employment in the hydrolysis of ammonia–borane (Zahmakiran et al. 2011; Rachiero et al. 2011; Akdim et al. 2013; Umegaki et al. 2009; Jiang et al. 2010a, b; Lu et al. 2012; Li et al. 2012; Umegaki et al. 2013).

At this concern, the recent studies have showed that hydroxyapatite ($[Ca_{10}(OH)_2(PO_4)_6]$, HAp) (Elliot 1994) can be used as suitable host support material for the guest metal(0) nanoparticles (Kaneda and Mizugaki 2009) because of its attractive features including; (i) structural nonporosity that reduces the mass transfer limitations in the catalytic reactions, (ii) high adsorption capacity through its ion-exchange sites, and (iii) low surface acidity, which prevents occuring of side reactions. These attractive properties of HAp stimulated us to use this support material in the stabilization of ligand-free metal(0) nanoparticles for the catalytic hydrolysis of ammonia–borane. In contrast to the previous studies, where micro-sized HAp (mean size >1 μm) have been used in the stabilization of Pd(0)NPs (Rakap and Özkar 2011), Co(0) (Rakap and Özkar 2012) and Ru(0) (Akbayrak et al. 2013) nanoparticles, in this study, we purposed that the employment of water-well-dispersed nano-sized HAp (60–150 nm), to stabilize ligand-free metal nanoparticles catalysts for the hydrolysis of ammonia–borane. We thought that the reduction of the particle size of HAp matrix from micro-size to nano-size regime (from >1 μm to ~100 nm) results in high external surface areas to guest metal nanoparticles, a larger number of exchange sites for the incorporation of metal precatalyst and lower mass transfer limitations in the catalytic hydrolysis of ammonia–borane in water (Tonbul et al. 2010; Zahmakiran et al. 2012).

In this study, we report, for the first time, our results on the preparation and characterization of palladium(0) nanoparticles dispersed in *nano*-HAp matrix, hereafter referred to as Pd(0)NPs/*n*-HAp, and their remarkable catalytic performance in terms of the ease preparation, catalytic activity, reusability, and lifetime for the hydrolysis of ammonia–borane at room temperature under air. Pd(0)NPs/*n*-HAp can simply and reproducibly be prepared by the ion-exchange of Pd(II) ions with Ca(II) ions of the *nano*-HAp matrix, followed by the in situ ammonia–borane reduction of Pd(II) ions within HAp matrix during the hydrolysis of ammonia–borane. The characterization of Pd(0)NPs/*n*-HAp was done by inductively coupled plasma-optical emission spectroscopy (ICP-OES), powder X-ray diffraction (P-XRD), conventional transmission electron microscopy (CTEM), and X-ray photoelectron spectroscopy (XPS), and the sum of their results is revealing that the formation of well-dispersed Pd(0)NPs (1.41 ± 0.52 nm) on the surface of *n*-HAp nanospheres (60–150 nm) by keeping the framework of host material intact. The resulting Pd(0)NPs/*n*-HAp catalyzes the hydrolysis of ammonia–borane at room temperature with an *initial* turnover frequency (TOF) of 11 min^{-1}. More importantly, *n*-HAp-dispersed palladium(0) nanoparticles provide superior stability against to agglomeration and leaching throughout the catalytic runs, which make them highly reusable and long-lived catalyst. Indeed, Pd(0)NPs/*n*-HAp retain 88 % of their initial catalytic activity even at 5th reuse and achieve 14,200 total turnovers in the hydrolysis of ammonia–borane.

Experimental

Materials

Synthetic hydroxyapatite nanocrystalline powder ($[Ca_5(OH)(PO_4)_3]_x$, ≥99.995 % trace metals basis), palladium(II) nitrate dihydrate ($Pd(NO_3)_2{\cdot}2H_2O$), ammonia–borane (NH_3BH_3, 97 %), D_2O, and BF_3-$(C_2H_5)_2O$ were purchased from Sigma-Aldrich. Deionized water was distilled with a water purification

system (Thermo Scientific Barnsted Nanopure System). All glassware and Teflon-coated magnetic stir bars were cleaned with acetone, followed by copious rinsing with doubly deionized water under ultrasonication, and finally dried in an oven at 150 °C.

Characterization

XRD data for *n*-HAp, Pd(II)/*n*-HAp, and Pd(0)NPs/*n*-HAp were collected using Rigaku X-ray diffractometer (Model, Miniflex) with Cu-Kα (30 kV, 15 mA, = 1.54051 Å) radiation at room temperature. TEM samples were prepared by dropping one drop of dilute suspension on copper-coated carbon TEM grid, and the solvent was then evaporated at room temperature under reduced pressure (10^{-3} torr). The conventional TEM was carried out on a JEOL JEM-200CX transmission electron microscopes operating at 120 kV. The palladium content of Pd(0)NPs/*n*-HAp was determined by inductively coupled plasma atomic emission spectroscopy (ICP-OES; ULTIMA 2-HORIBA Jobin–Yvon) after the powdered sample was completely dissolved in the mixture of aqua regia (HNO_3:HCl in a 1:3 ratio). The nitrogen adsorption/desorption experiments were carried out at 77 K using a NOVA 3000 series (Quantachrome Inst.) instrument. The sample was outgassed under vacuum at 393 K for 3 h before the adsorption of nitrogen. XPS analysis was performed on a Kratos AXIS ultra imaging X-ray photoelectron spectrometer using monochromatic Al Kα radiation (1486.6 eV, the X-ray tube working at 15 kV, 350 W and pass energy of 23.5 keV). At the end of the hydrolysis reaction, the resulting solutions were filtered and the filtrates were collected for ^{11}B NMR analysis. ^{11}B NMR spectra were recorded on a Bruker Avance DPX 400 with an operating frequency of 128.15 MHz. D_2O and $BF_3{\cdot}(C_2H_5)_2O$ were used as a lock and an external reference, respectively.

Preparation of palladium(II)-exchanged nanohydroxyapatite (Pd(II)/n-HAp) precatalyst and the general procedure for the in situ generation of palladium(0) nanoparticles dispersed in nanohydroxyapatite (Pd(0)NPs/n-HAp) framework plus testing their activity in the hydrolysis of ammonia–borane

Palladium(II) cations were introduced into Ca(II)/*n*-HAp by the ion-exchange of 200 mg of Ca(II)/*n*-HAp in 10 mL of an aqueous solution of 20.9 mg of $Pd(NO_3)_2{\cdot}2H_2O$ (0.08 mmol) for 12 h at room temperature. The sample was then filtered by suction filtration using a filter paper (Whatman-1), washed three times with 100 mL of deionized water, and dried at 80 °C in the oven. The in situ formation of Pd(0)NPs/*n*-HAp and the concomitant hydrolysis of ammonia–borane were performed in a typical jacketed, three-necked reaction flask thermostatted at 25 ± 0.1 °C and connected to the water-filled cylinder glass tube. In a typical experiment, 33 mg of Pd(II)/*n*-HAp (with 3.2 wt% Pd loading corresponding to 10.0 μmol Pd) was weighted and placed into a reaction flask containing a new 5/16 in ×5/8 in stir bar. Next, 10.0 mL of 100 mM AB solution was added to the reaction flask, the reaction timer was started ($t = 0$ min) and started to stirring at 900 rpm. Hydrogen gas generation from the catalytic reaction solution was followed using a typical water-filled gas buret system and recording the displacement of the water level in the gas buret until no more hydrogen evolution was observed. When no more hydrogen generation was observed, the experiment was stopped, the reactor was disconnected from the water-filled tube, and the hydrogen pressure was released and a small aliquot from the reaction solution in the culture tube was withdrawn for ^{11}B NMR analysis.

Testing the isolability and reusability of Pd(0)NPs/*n*-HAp in the hydrolysis of ammonia–borane

After the first run of the Pd(0)NPs/*n*-HAp (10.0 μmol Pd)-catalyzed hydrolysis of ammonia–borane (1.0 mmol NH_3BH_3 in 10 mL H_2O) at 25 ± 0.1 °C, the catalyst was isolated by suction filtration, washed three times with 20 mL of deionized water, and dried under N_2 gas purging at room temperature. The dried samples of Pd(0)NPs/*n*-HAp were weighted and used again in the hydrolysis of 100 mM ammonia–borane in 10 mL H_2O and the same procedure was repeated up to 5th catalytic cycle. The results were expressed as percentage of the retained initial catalytic activity of Pd(0)NPs/*n*-HAp in the hydrolysis of ammonia–borane versus number of catalytic runs.

Determination of the catalytic lifetime of Pd(0)NPs/*n*-HAp in the hydrolysis of ammonia–borane

The catalytic lifetime of Pd(0)NPs/*n*-HAp formed in situ during the hydrolysis of ammonia–borane was

determined by measuring total turnover number (TTON). This experiment was started with 33 mg of Pd(II)/*n*-HAp (with 3.2 wt% Pd loading corresponding to 10.0 μmol Pd) precatalyst in a 20 mL solution of 100 mM ammonia–borane. When all the ammonia–borane in the solution was completely hydrolyzed, more AB was added, and the reaction was continued in this way until no hydrogen gas evolution was observed.

Results and discussion

The preparation and characterization of palladium(0) nanoparticles supported on hydroxyapatite nanospheres

Pd(0)NPs/*n*-HAp can simply and reproducibly be prepared by the ion-exchange of Pd^{2+} ions with extra framework Ca^{2+} ions of *n*-HAp matrix, followed by reduction of Pd^{2+} ions within the framework of *n*-HAp with ammonia–borane in aqueous solution during the hydrolysis of ammonia–borane. The catalyst formation and concomitant hydrolysis usually follow two-steps, slow nucleation and then autocatalytic surface growth mechanism (Çalışkan, et al. 2013; Zahmakiran and Özkar 2009), A → B (**1**) and A + B→2B (**2**), in which A is Pd^{2+}@*n*-HAp and B is the growing, catalytically active Pd(0)NPs/*n*-HAp.

$$A \xrightarrow{k_1} B \quad (2)$$

$$A + B \xrightarrow{k_2} 2B \quad (3)$$

Figure 1 shows P-XRD patterns of the host material *n*-HAp, Pd^{2+}-exchanged-*n*-HAp, (Pd(II)/*n*-HAp) and Pd(0)NPs/*n*-HAp altogether. A comparison of the P-XRD patterns undoubtedly reveals that the integration of palladium(II) ions into *n*-HAp and the reduction of palladium(II) ions forming the palladium(0) nanoparticles within *n*-HAp matrix cause no observable alteration in the framework lattice and no lost in the crystallinity of *n*-HAp. The decrease in the intensity of Bragg peaks in Pd(0)NPs/*n*-HAp can be explained by the changes in the charge distribution and electrostatic fields as result of the existence of Pd(0) nanoparticles on the surface (vide infra) and interaction of their electrophilic surface with framework oxygen atoms (Zahmakiran et al. 2012).

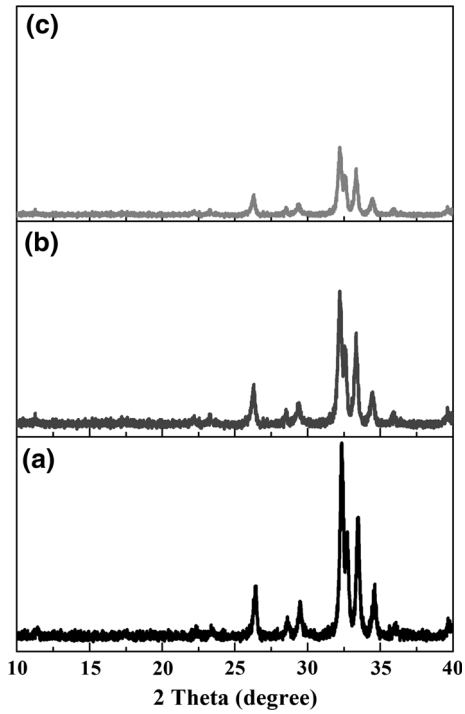

Fig. 1 The P-XRD patterns of **a** nanohydroxyapatite (*n*-HAp), **b** palladium(II)-exchanged nanohydroxyapatite (Pd(II)/*n*-HAp) and **c** palladium(0) nanoparticles stabilized by nanohydroxyapatite framework (Pd(0)NPs/*n*-HAp)

The composition and morphology of Pd(0)NPs/*n*-HAp were investigated by CTEM and ICP-OES analyses. Figure 2a–c shows the CTEM images (in different magnifications) of Pd(0)NPs/*n*-HAp with palladium loading of 3.2% (as determined by ICP-OES), which reveal that the existence of palladium(0) nanoparticles with an average diameter of 1.41 ± 0.52 nm (Fig. 2d) on the hydroxyapatite nanospheres and agglomerates (60–150 nm).

The oxidation state of palladium in the Pd(0)NPs/*n*-HAp sample was investigated by X-ray photoelectron spectroscopy (XPS). Figure 3 shows high-resolution Pd 3d XPS spectrum and its curve fitting of Pd(0)NPs/*n*-HAp, which gives two prominent peaks at 335.8 and 341.2 eV, readily assigned to Pd(0)NPs $3d_{5/2}$ and Pd(0)NPs $3d_{3/2}$, respectively (Evangelisti et al. 2009). Two satellite peaks observed around 338.3 and 343.5 eV can be assigned to Pd(II) $3d_{5/2}$ and Pd(II) $3d_{3/2}$ and indicative of the surface oxidation of resulting Pd(0)NPs/*n*-HAp during the XPS sampling procedure (Evangelisti et al. 2009).

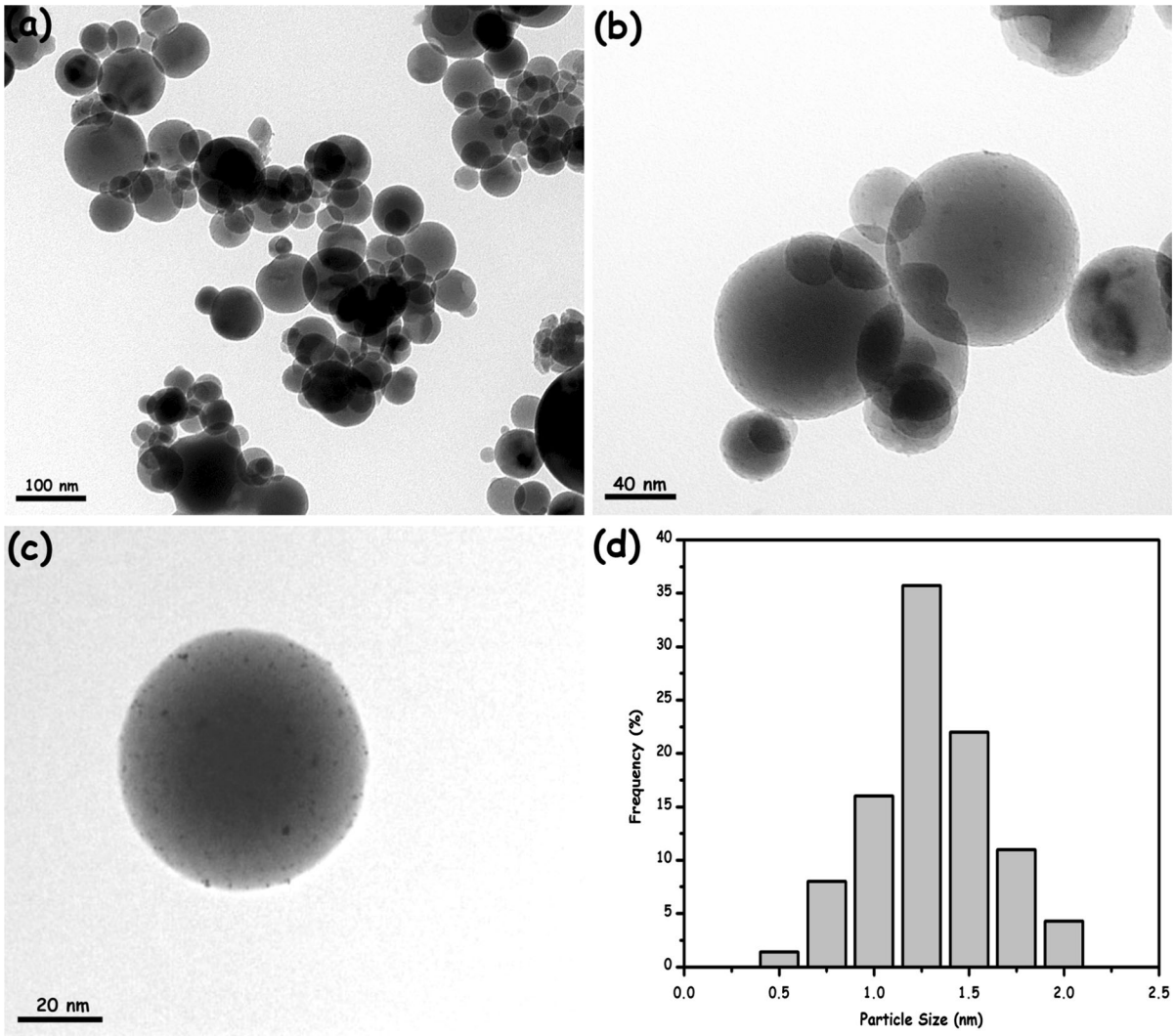

Fig. 2 **a–c** are the CTEM images of palladium(0) nanoparticles stabilized by nanohydroxyapatite framework (Pd(0)NPs/*n*-HAp) in different magnifications, and **d** the size histogram of nanohydroxyapatite-supported Pd(0) nanoparticles

Nitrogen adsorption–desorption isotherms of *n*-HAp and Pd(0)NPs/*n*-HAp (3.2 wt% Pd loading) are given in Fig. 4 and both of them show Type III shape, reflecting the absence of micropores (<2 nm) (Storck et al. 1998). The Brunauer–Emmett–Teller (BET) surface area of Pd(0)NPs/*n*-HAp was found to be 40 m^2/g, which is larger than that of the parent *n*-HAp (25 m^2/g). This result accounts for the physical adsorption of palladium(0) nanoparticles on the nanohydroxyapatite surface. Furthermore, no hysteresis loop was observed in the N_2 adsorption–desorption isotherm of Pd(0)NPs/*n*-HAp, indicating that the procedure followed in the preparation of Pd(0)NPs/*n*-HAp does not create any mesopores within the framework of *n*-HAp framework.

The catalytic performance of in situ-generated palladium(0) nanoparticles supported on hydroxyapatite nanospheres in the hydrolysis of ammonia–borane

In the determination of the catalytic activity of Pd(0)NPs/*n*-HAp accurately one has to check whether *n*-HAp catalyzes the hydrolysis of ammonia–borane. The hydrolysis of ammonia–borane in the presence of *n*-HAp was performed at various temperatures in the

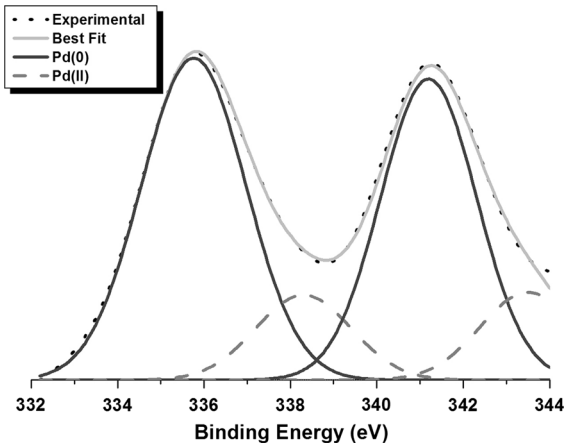

Fig. 3 Experimental and simulated high-resolution Pd 3d XPS spectrum of palladium(0) nanoparticles stabilized by nanohydroxyapatite framework (Pd(0)NPs/*n*-HAp)

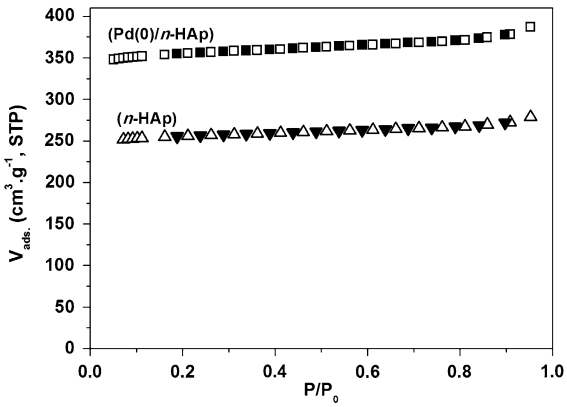

Fig. 4 Nitrogen adsorption–desorption isotherms of nanohydroxyapatite (*n*-HAp) (*down*) and palladium(0) nanoparticles stabilized by nanohydroxyapatite framework (Pd(0)NPs/*n*-HAp) (*up*)

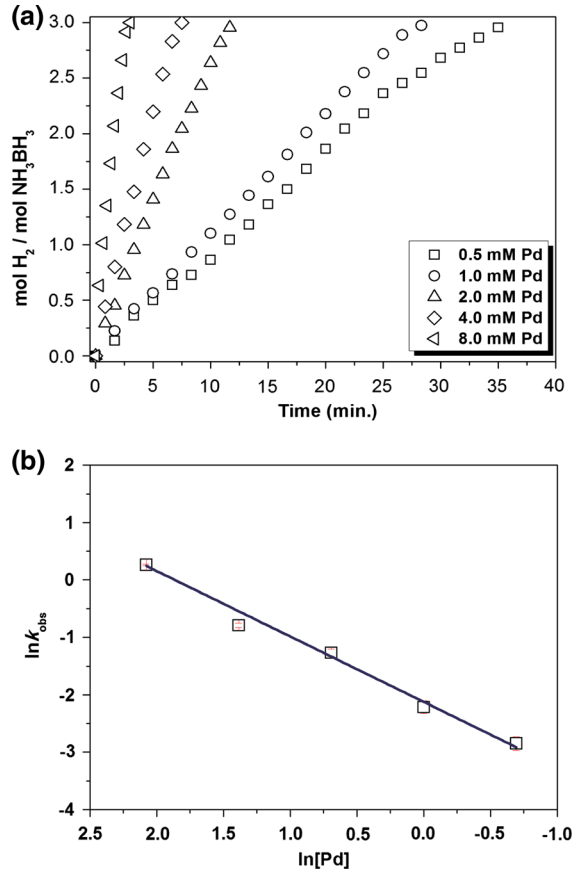

Fig. 5 **a** Plot of mol of H_2 generated per mol of NH_3BH_3 versus time (min) for the in situ-generated Pd(0)NPs/*n*-HAp-catalyzed hydrolysis of ammonia–borane starting with Pd(II)/*n*-HAp precatalysts with different Pd concentrations as given on the graph (in all $[NH_3BH_3] = 100$ mM in 10.0 mL H_2O) at 25 ± 0.1 °C, **b** ln k_{obs} versus ln [Pd] graph for the in situ-generated Pd(0)NPs/*n*-HAp-catalyzed hydrolysis of ammonia–borane

range of 25–45 °C (25, 30, 35, 40, and 45 °C) and found that the host material *n*-HAp causes no hydrogen generation even at 45 °C. The hydroxyapatite-supported palladium(0) nanoparticles formed in situ were found to be highly active catalyst in the hydrolysis of ammonia–borane. Figure 5a shows the plots of the stoichiometric ratio of generated H_2 to NH_3BH_3 versus time during the catalytic hydrolysis of 100 mM NH_3BH_3 solution starting with Pd(II)/*n*-HAp precatalyst (with 3.2 wt% Pd loading) in different palladium concentrations at 25 ± 0.1 °C. As a result of fast reduction of Pd(II) to Pd(0)NPs without an induction time period, a linear hydrogen generation starts immediately and continues until completion. For example, using Pd(0)NPs/*n*-HAp in 0.5 mM Pd concentration leads to a complete hydrogen release (3.0 mol H_2/NH_3BH_3) within 37 min at 25 ± 0.1 °C. In addition to the volumetric measurement of the hydrogen gas evolution, the completion of catalytic hydrolysis was also ascertained by ^{11}B NMR spectroscopy. At the end of the catalytic reaction, the signal of NH_3BH_3 at $\delta = -24.3$ ppm (q) (Fig. 6a) completely disappears and a new resonance at $\delta = 9.0$ ppm (s) (Fig. 6b) shows up, which is readily assigned to metaborate anion (Ramachandran and Gagare 2007). The quantity of ammonia liberated during the hydrolysis of ammonia–borane has been found to be negligible when the catalyst concentration

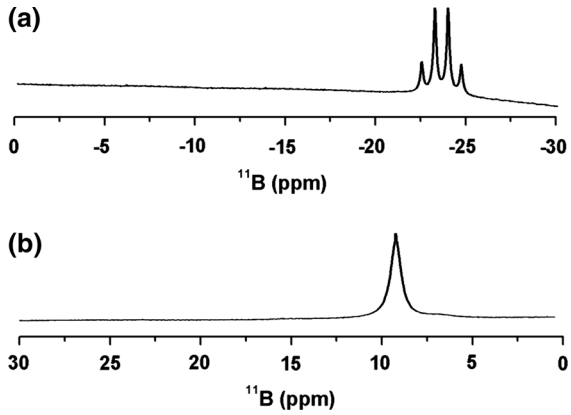

Fig. 6 ^{11}B NMR spectra of **a** NH_3BH_3 solution, **b** the aliquot taken from the reaction solution at the end of the in situ-generated Pd(0)NPs/*n*-HAp-catalyzed hydrolysis of ammonia–borane

is less than 0.07 mol% and the substrate concentration is lower than 8 wt% (Ramachandran and Gagare 2007). We performed the control tests using copper(II) sulfate and acid/base indicator, the sum of their results showed no ammonia evolution in detectable amount. The hydrogen generation rate was determined from the linear portion of the plot for each experiment with different palladium concentrations (k_{obs} = 0.092, 0.109, 0.281, 0.453, and 1.304 mmol H_2/min for 0.5, 1.0, 2.0, 4.0, and 8.0 mM Pd concentrations, respectively). The graph in Fig. 5b shows the plot of hydrogen generation rate versus catalyst concentration, both on logarithmic scales. One obtains a straight line, the slope of which is found to be 1.03–1.0 within experimental error. This result indicates that the catalytic hydrolysis of ammonia–borane is first order with respect to the palladium concentration.

The effect of substrate concentration on the hydrogen generation rate was also studied by performing a series of experiments starting with varying initial concentration of ammonia–borane, while keeping the palladium concentration constant at 1.0 mM. Figure 7a shows the plot of hydrogen volume versus time for various ammonia–borane concentrations. The hydrogen generation rate determined from the linear portion of the plot for each experiment (k_{obs} = 0.089, 0.099, 0.109, 0.114, and 0.124 mmol H_2/min for 50, 75, 100, 125, and 150 mM AB concentrations, respectively) was plotted against the substrate concentration, both axes on the logarithmic scale, as given

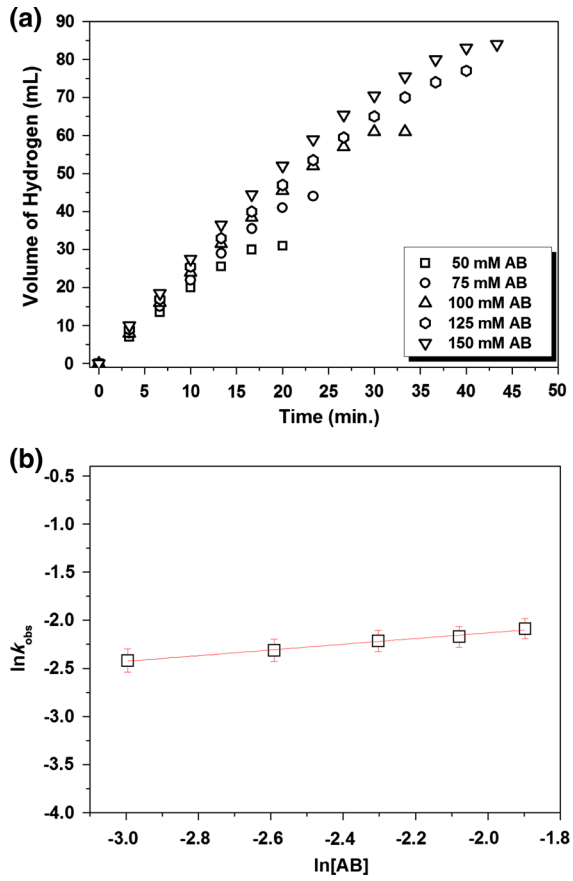

Fig. 7 **a** Plot of mol of H_2 generated per mol of NH_3BH_3 versus time (min) for the in situ-generated Pd(0)NPs/*n*-HAp-catalyzed hydrolysis of ammonia–borane starting with Pd(II)/*n*-HAp precatalysts at different NH_3BH_3 concentrations as given on the graph (in all [Pd] = 1.0 mM in 10.0 mL H_2O) at 25 ± 0.1 °C, **b** ln k_{obs} versus ln [NH_3BH_3] graph for the in situ-generated Pd(0)NPs/*n*-HAp-catalyzed hydrolysis of ammonia–borane

in Fig. 7b. The slope of the straight line is almost zero indicating that the catalytic hydrolysis is zero order with respect to substrate concentration.

Thus, the rate law for the hydrolysis of ammonia–borane catalyzed by in situ-generated Pd(0)NPs/*n*-HAp can be given as by (Eq. (2)):

$$-\frac{d[NH_3BH_3]}{dt} = +\frac{d[H_2]}{3dt} = k_{obs}[Pd] \quad (4)$$

Figure 8a shows the stoichiometric ratio of generated H_2 to NH_3BH_3 versus time during the catalytic hydrolysis of 100 mM NH_3BH_3 solution starting with Pd(II)/*n*-HAp ([Pd] = 1.0 mM) precatalyst (with 3.2 wt% Pd loading) at various temperatures (25, 35,

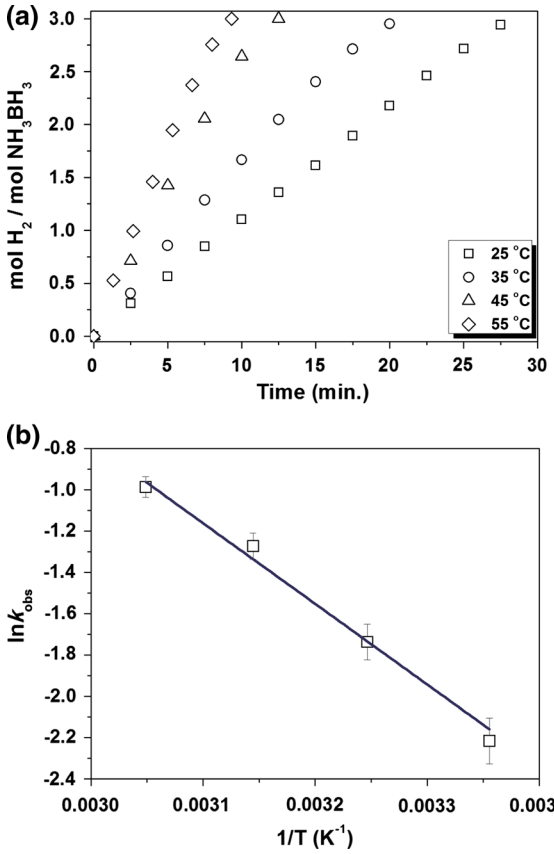

Fig. 8 **a** Plot of mol of H_2 generated per mol of NH_3BH_3 versus time (min) for the in situ-generated Pd(0)NPs/*n*-HAp-catalyzed hydrolysis of ammonia–borane starting with Pd(II)/*n*-HAp precatalysts at different temperatures as given on the graph (in all [Pd] = 1.0 mM, [NH_3BH_3] = 100 mM in 10.0 mL H_2O), **b** Arrhenius plot for the in situ-generated Pd(0)NPs/*n*-HAp-catalyzed hydrolysis of ammonia–borane

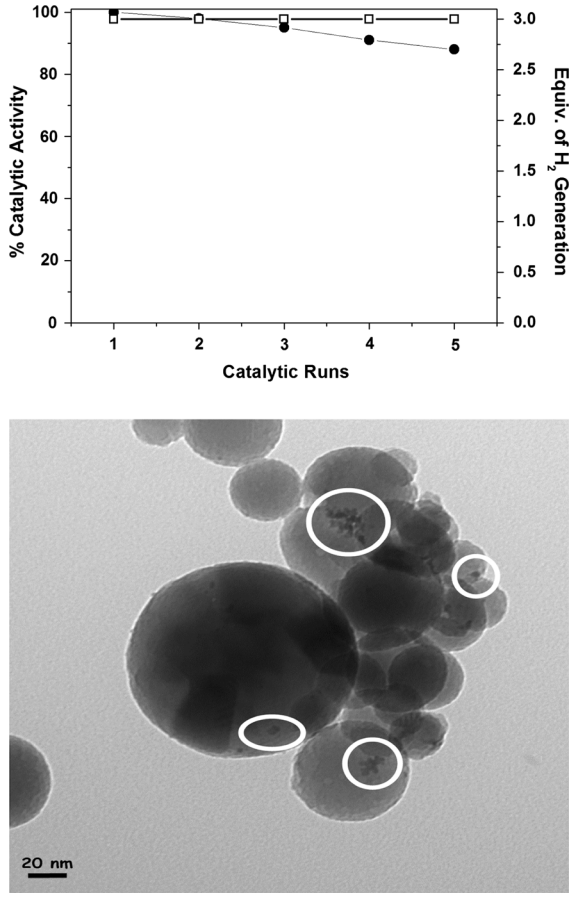

Fig. 9 Plot of % initial catalytic activity (retained) mol^{-1} of H_2 generated per mol of NH_3BH_3 versus catalytic runs for testing reusability of in situ-generated Pd(0)NPs/*n*-HAp in the catalytic hydrolysis of ammonia–borane. CTEM image of Pd(0)NPs/*n*-HAp sample harvested after the fifth run of hydrolysis of ammonia–borane (*white circles* show slightly agglomerated Pd NPs)

45 and 55 °C). The rate constants of hydrogen generation from the catalytic hydrolysis of ammonia–borane were measured as 0.109, 0.176, 0.280, and 0.373 mmol H_2/min from the linear portions of the plots given in Fig. 8a for 25, 35, 45, and 55 °C, respectively. These obtained rate constants were then used for the calculation of activation energy (E_a = 32.5 kJ mol^{-1}) from the Arrhenius plot given in Fig. 8b.

Pd(0)NPs/*n*-HAp were also tested for their isolability and reusability in the ammonia–borane hydrolysis. After the complete hydrolysis of ammonia–borane solution catalyzed by Pd(0)NPs/*n*-HAp at room temperature, the catalyst was isolated as powders by drying in vacuum and then bottled under inert atmosphere. The isolated sample of Pd(0)NPs/*n*-HAp is redispersible in aqueous solution and yet active catalyst in the hydrolysis of ammonia–borane. Figure 9 shows the changes in the percentage of initial activity in the successively repeated hydrolysis, isolation, and redispersion cycles at 25 ± 0.1 °C. They retain >85 % of their initial activity at the fifth catalytic run in the hydrolysis of ammonia–borane with 3 equiv. of H_2 generation. This result is indicative of Pd(0)NPs/*n*-HAp are isolable, bottleable, and redispersible and yet catalytically active catalyst. In other words, they can be repeatedly used as active catalyst in the hydrolysis of ammonia–borane. The slight decrease in catalytic activity of Pd(0)NPs/*n*-

HAp in following runs can be attributed to (i) blockage of nanoparticles surface by metaborate anion, which decreases accessibility of Pd active sites (Jaska et al. 2005), and (ii) decrease in the number of active surface atoms due to the clumping of surface bound Pd NPs as evidenced by CTEM image of Pd(0)NPs/*n*-HAp (Fig. 9) sample harvested after the fifth run of hydrolysis of ammonia–borane.

Moreover, Pd was not detected in the filtrate by the ICP technique confirms the retention of palladium within the *n*-HAp matrix (no palladium passes into the solution during the suction filtration). A control experiment was also performed to show that the catalytic hydrolysis of ammonia–borane is completely stopped by the removal of Pd(0)NPs/*n*-HAp from the reaction solution. A catalyst lifetime experiment starting with 1.0 mM Pd(0)NPs/*n*-HAp and 200 mM of ammonia–borane at 25 ± 0.1 °C reveals a total turnover (TTO) value of 14200 in the hydrolysis of ammonia–borane over 33 h before deactivation. An initial TOF value of 11 min^{-1} was obtained; however, the average TOF value was calculated to be 7 min^{-1}. The observation that the TOF value decreases as the reaction proceeds indicates the deactivation of the palladium(0) nanoparticles catalyst.

In summary, the comparison of the catalytic performance of Pd(0)NPs/*n*-HAp with the previous Pd-based catalyst systems (Rakap and Özkar 2011; Metin et al. 2009; Rakap and Özkar 2010; Rakap et al. 2012; Kiliç et al. 2012; Xi et al. 2012) tested in the hydrolysis of ammonia–borane showed that Pd(0)NPs/*n*-HAp provide notable activity, durability, and lifetime in this important catalytic reaction.

Conclusions

Pd(0)NPs/*n*-HAp were successfully employed as catalyst in the hydrolysis of ammonia–borane , which has been considered as a promising hydrogen storage material. Pd(0)NPs/*n*-HAp are easily prepared at room temperature by ion-exchange of Pd^{2+} ions with the extra framework Ca^{2+} ions in nano-sized-hydroxyapatite (*n*-HAp), followed by the in situ reduction of the Pd^{2+} ions within the matrix of *n*-HAp with ammonia–borane in aqueous solution. Since active sites of Pd(0)NPs/*n*-HAp are free from capped ligands and/or polymers, which are used for synthesis of water dispersible colloidal metal nanocatalysts, they act as highly active catalyst in the hydrolysis of ammonia–borane. They provide TTO of 14200 and an initial TOF of 11 min^{-1} in the hydrolysis of ammonia–borane at room temperature. These values are higher than those of found by micro-sized HAp-supported Pd NPs (TTO = 12300 and TOF = 6.8 min^{-1}), (Rakap and Özkar 2011), which reveals that the reduction of the particle size of HAp matrix from micro-size to nano-size regime (from >1 μm to ~100 nm) results in higher activity for the guest Pd nanoparticles in the hydrolysis of ammonia–borane. The interaction between host *n*-HAp matrix and guest Pd NPs was found to be enough to prevent surface agglomeration of Pd NPs and the leaching of Pd NPs into reaction solution, which make them highly reusable catalytic material in the hydrolysis of ammonia–borane. They retain almost their inherent catalytic activity (>85 % of their initial activity) even at the fifth catalytic run for the hydrolysis of ammonia–borane. The complete release of hydrogen is achieved even in successive runs performed by redispersing the Pd(0)NPs/*n*-HAp isolated after the previous run. Thus, Pd(0)NPs/*n*-HAp can be used as isolable, bottleable, and redipersible heterogeneous catalyst in the hydrolysis of ammonia–borane.

References

Akbayrak S et al (2013) Hydroxyapatite supported ruthenium(0) nanoparticles catalyst in hydrolysis of ammonia borane: insight to the nanoparticles formation and hydrogen evolution kinetics. App Catal B 142:187–195

Akdim O et al (2013) A bottom-up approach to prepare cobalt-based bimetallic supported catalysts for hydrolysis of ammonia borane. Int J Hydrog Energy 38:5627–5637

Bluhm ME et al (2006) Amineborane-based chemical hydrogen storage: enhanced ammonia borane dehydrogenation in ionic liquids. J Am Chem Soc 128:7748–7749

Çalışkan et al (2012) Hydrogen liberation from the hydrolytic dehydrogenation of dimethylamine–borane at room temperature by using a novel ruthenium nanocatalyst. Dalton Trans 41:4976–4984

Ciganda R et al (2010) A hydridoirida-β-diketone as an efficient and robust homogeneous catalyst for the hydrolysis of ammonia–borane or amine–borane adducts in air to produce hydrogen. Dalton Trans 39:7226–7229

Demirci UB, Miele P (2009) Sodium borohydride versus ammonia borane, in hydrogen storage and direct fuel cell applications. Energy Environ Sci 2:627–637

Demirci UB et al (2011) Hydrogen release by thermolysis of ammonia borane NH_3BH_3 and then hydrolysis of its by-product [BNH_x]. J Power Sources 196:279–286

Dixon DA, Gutowski M (2005) Thermodynamic properties of molecular borane amines and the $[BH_4^-][NH_4^+]$ salt for chemical hydrogen storage systems from ab initio electronic structure theory. J Phys Chem A 109:5129

Durap F et al (2009a) Water soluble laurate-stabilized ruthenium(0) nanoclusters catalyst for hydrogen generation from the hydrolysis of ammonia–borane : high activity and long lifetime. Int J Hydrog Energy 34:7223–7230

Durap F et al (2009b) Water soluble laurate-stabilized rhodium(0) nanoclusters catalyst: unprecedented catalytic lifetime in the hydrolysis of ammonia–borane. App Catal A 369:53–59

Elliot JC (1994) Structure and chemistry of apatites and other calcium orthophosphates. Elsevier, Amsterdam

Evangelisti C et al (2009) Palladium nanoparticles supported on polyvinylpyridine: catalytic activity in Heck-type reactions and XPS structural studies. J Catal 262:287–293

Graham TW et al (2010) Catalytic solvolysis of ammonia borane. Angew Chem Int Ed 49:8708–8711

Hamilton CW et al (2009) B–N compounds for chemical hydrogen storage. Chem Soc Rev 38:279–293

Inter Academy Council (2007) Lighting the way towards a sustainable energy futures. Inter Academy Council (IAC) Report, Amsterdam

Jaska CA et al (2003) Transition metal-catalyzed formation of boron–nitrogen bonds: catalytic dehydrocoupling of amine–borane adducts to form aminoboranes and borazines. J Am Chem Soc 125:9424–9434

Jaska CA et al (2005) Poisoning of heterogeneous, late transition metal dehydrocoupling catalysts by boranes and other group 13 hydrides. J Am Chem Soc 127:5116–5124

Jiang HL, Xu Q (2011) Catalytic hydrolysis of ammonia borane for chemical hydrogen storage. Catal Today 170:56–63

Jiang H-L et al (2010a) Bimetallic Au–Ni nanoparticles embedded in SiO_2 nanospheres: synergetic catalysis in hydrolysis of ammonia borane. Chem A Eur J 16:3132–3137

Jiang HL et al (2010b) Liquid-phase chemical hydrogen storage: catalytic hydrogen generation under ambient conditions. ChemSusChem 3:541–549

Kaneda K, Mizugaki T (2009) Development of concerto metal catalysts using apatite compounds for green organic syntheses. Energy Environ Sci 2:655–673

Kiliç B et al (2012) Hydrolysis of ammonia borane catalyzed by reduced graphene oxide supported monodisperse palladium nanoparticles: high activity and detailed reaction kinetics. J Mol Catal A 361:104–110

Li P-Z et al (2012) ZIF-8 immobilized nickel nanoparticles: highly effective catalysts for hydrogen generation from hydrolysis of ammonia borane. Chem Commun 48:3173–3175

Liu C et al (1999) Hydrogen storage in single-walled carbon nanotubes at room temperature. Science 286:1127–1129

Lu Z-H et al (2012) Synergistic catalysis of Au–Co@SiO_2 nanospheres in hydrolysis of ammonia borane for chemical hydrogen storage. J Mat Chem 22:5065–5071

McKeown NB, Budd PM (2006) Polymers of intrinsic microporosity (PIMs): organic materials for membrane separations, heterogeneous catalysis and hydrogen storage. Chem Soc Rev 35:675–683

Metin O et al (2009) Water-soluble poly(4-styrenesulfonic acid-*co*-maleic acid)-stabilized ruthenium(0) and palladium(0) nanoclusters as highly active catalysts in hydrogen generation from the hydrolysis of ammonia–borane. Int J Hydrog Energy 34:6304–6313

Moussa G et al (2013) Boron-based hydrides for chemical hydrogen storage. Int J Energ Res 37:825–842

Muradova NZ, Veziroglu TN (2005) From hydrocarbon to hydrogen–carbon to hydrogen economy. Int J Hydrog Energy 30:225–237

National Academy of Engineering (2004) The hydrogen economy: opportunities, costs, barriers, and R&D needs. The National Academies Press, Washington

Ogden JM (1999) Developing an infrastructure for hydrogen vehicles: a Southern California case study. Int J Hydrog Energy 24:709–730

Rachiero GP et al (2011) Bimetallic RuCo and RuCu catalysts supported on γ-Al_2O_3: a comparative study of their activity in hydrolysis of ammonia–borane. Int J Hydrog Energy 36:7051–7065

Rakap M, Özkar S (2010) Hydrogen generation from the hydrolysis of ammonia–borane using intrazeolite cobalt(0) nanoclusters catalyst. Int J Hydrog Energy 35:1305–1312

Rakap M, Özkar S (2011) Hydroxyapatite-supported palladium(0) nanoclusters as effective and reusable catalyst in hydrogen generation from the hydrolysis of ammonia–borane. Int J Hydrog Energy 36:7019–7027

Rakap M, Özkar S (2012) Hydroxyapatite-supported cobalt(0) nanoclusters as efficient and cost-effective catalyst for hydrogen generation from the hydrolysis of both sodium borohydride and ammonia–borane. Catal Today 183: 17–25

Rakap M et al (2012) Hydrogen generation from hydrolysis of ammonia–borane using Pd–PVB–TiO_2 and Co–Ni–P/Pd–TiO_2 under stirred conditions. J Power Sources 210: 184–190

Ramachandran PV, Gagare PD (2007) Preparation of ammonia borane in high yield and purity, methanolysis, and regeneration. Inorg Chem 46:7810–7817

Rosi NL et al (2003) Hydrogen storage in microporous metal–organic frameworks. Science 300:1127–1129

Sanyal U et al (2011) Hydrolysis of ammonia borane as hydrogen source, fundamental issues and potential solutions towards implementation. ChemSusChem 4:1731–1739

Staubitz A et al (2010) Ammonia–borane and related compounds as dihydrogen sources. Chem Rev 110:4079–4124

Stephens FH et al (2007) Ammonia–borane: the hydrogen source par excellence? Dalton Trans 25:2613–2626

Storck S et al (1998) Characterization of micro- and mesoporous solids by physisorption methods and pore-size analysis. App Catal A 174:137–146

Thomas JM, Thomas WJ (1997) Principles and practice of heteregeneous catalysis.VCH, New York

Toche F et al (2012) Ammonia borane thermolytic decomposition in the presence of metal (II) chlorides. Int J Hydrog Energy 37:6749–6755

Tonbul Y et al (2010) Monodisperse nickel nanoparticles and their catalysis in hydrolysis of ammonia borane. J Am Chem Soc 132:6541

Turner JA (1999) A realizable renewable energy future. Science 285:687–689

Turner J et al (2008) Renewable hydrogen production. Int J Energy Res 32:379–407

Umegaki T et al (2009) Hollow Ni–SiO_2 nanosphere-catalyzed hydrolysis of ammonia borane for chemical hydrogen storage. J Power Sources 191:209–216

Umegaki T et al (2013) Fabrication of hollow nickel-silica composite spheres using L(+)-arginine and their catalytic performance for hydrolysis of ammonia borane. J Mol Catal A 371:1–7

Weitkamp J et al (1995) Zeolites as media for hydrogen storage. Int J Hydrog Energy 20:967–970

Xi P et al (2012) Surfactant free RGO/Pd nanocomposites as highly active heterogeneous catalysts for the hydrolysis of ammonia borane for chemical hydrogen storage. Nanoscale 4:5597–5601

Zahmakiran M, Özkar S (2009) Dimethylammonium hexanoate stabilized rhodium(0) nanoclusters identified as true heterogeneous catalysts with the highest observed activity in the dehydrogenation of dimethylamine–borane. Inorg Chem 48:8955–8964

Zahmakiran M, Özkar S (2011) Metal nanoparticles in liquid phase catalysis; from recent advances to future goals. Nanoscale 3:3462–3481

Zahmakiran M et al (2011) Zeolite framework stabilized nickel(0) nanoparticles: active and long-lived catalyst for hydrogen generation from the hydrolysis of ammonia–borane and sodium borohydride. Catal Today 170:76–84

Zahmakiran M et al (2012) Rhodium(0) nanoparticles supported on nanocrystalline hydroxyapatite: highly effective catalytic system for the solvent-free hydrogenation of aromatics at room temperature. Langmuir 28:60–64